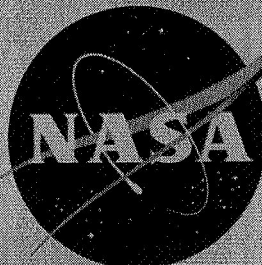


Copy

NASA TM X-464

547

NASA TM X-464



UNCLASSIFIED

J.D. 4635 10/18/91

TECHNICAL MEMORANDUM

X-464

Declassified by authority of NASA
Classification Office Access No. 215
Dated ** 12/31/77

TESTS OF AN INTERNAL-COMPRESSION INDUCTION SYSTEM WITH
INLETS LOCATED ON OPPOSITE SIDES OF AN AIRPLANE
FUSELAGE AT MACH NUMBERS FROM 1.72 TO 2.50

By Walter A. Vahl and Waldo I. Oehman

Langley Research Center
Langley Field, Va.

FACILITY FORM 602

(ACCESSION NUMBER)

35

(PAGES)

N71-75597

(THRU)

None

(CODE)

(NASA CR OR TMX OR AD NUMBER)

(CATEGORY)

NATIONAL AERONAUTICS AND SPACE ADMINISTRATION
WASHINGTON

April 1961

CONFIDENTIAL

[REDACTED]

NATIONAL AERONAUTICS AND SPACE ADMINISTRATION

TECHNICAL MEMORANDUM X-464

TESTS OF AN INTERNAL-COMPRESSION INDUCTION SYSTEM WITH
INLETS LOCATED ON OPPOSITE SIDES OF AN AIRPLANE
FUSELAGE AT MACH NUMBERS FROM 1.72 TO 2.50*

By Walter A. Vahl and Waldo I. Oehman

SUMMARY

An investigation has been conducted in the Langley Unitary Plan wind tunnel to determine the pressure recovery, mass-flow ratio, and distortion parameter of a variable-geometry induction system with translating central bodies and with two circular inlets located on opposite sides of a fuselage. The induction system was designed for a Mach number of 2.50. Supersonic compression was conical and internal. The tests were made with a basic fuselage, a faired-canopy fuselage, and a flat-plate model. In addition, tests were made for several boundary-layer removal systems and for a canard control at deflection angles of 1.5° , 5.5° , and 9.5° .

The Mach number range of the tests was from 1.72 to 2.50. The Reynolds number range was from 2.5×10^6 to 4.4×10^6 based on a length of 1 foot. Fuselage angle of attack was varied from -4° to 10° .

Boundary-layer removal forward of the duct minimum section was necessary in order to approach the desired flow characteristics. At the design Mach number, the maximum pressure recovery obtained with the basic fuselage was 0.76 and occurred at an angle of attack of 3° . For the faired-canopy fuselage, the maximum pressure recovery at the design Mach number was 0.80 and occurred at an angle of attack of 1.5° .

The mass-flow ratio and distortion parameter were the same for the two fuselages at angles of attack between 0° and 4° . The canard control at a deflection angle of 1.5° had no appreciable effect on the internal-flow characteristics of the induction system.

[REDACTED]

[REDACTED]

INTRODUCTION

Most experimental investigations of induction systems have been conducted with the inlet in uniform flow. (See refs. 1 to 4.) The performance of an induction system may be greatly altered whenever the inlet is in the interfering flow field generated by an airplane fuselage. (See ref. 5.) Furthermore, the effect on performance would be different for each fuselage shape. Consequently, the induction-system performance for a particular airplane must be determined individually.

An experimental investigation has been conducted in the Langley Unitary Plan wind tunnel to determine the internal-flow characteristics of the induction system of a fighter-type airplane model. The system had two circular inlets located on opposite sides of the fuselage. Supersonic compression was conical and internal. A movable central body provided variable duct geometry for starting and for variable Mach number operation. Bleeding of boundary-layer air from internal surfaces was provided by perforations vented to the local free stream.

The tests were made at Mach numbers ranging from 1.72 to 2.50 and at angles of attack ranging from -4° to 10° . For some of the tests, the canopy was faired into the forward part of the fuselage. In addition, some tests were made with the fuselage replaced by flat plates. Furthermore, the effect of a canard control was determined for several deflection angles. The number and location of perforations for removal of the boundary layer also were varied.

Because of limited applicability, the test results are presented with a minimum of analysis.

SYMBOLS

$\frac{A_2}{A_1}$	area ratio (ratio of local duct area to inlet area)
M	free-stream Mach number
p_t	total pressure, lb/sq ft abs
$p_{t,r}$	total-pressure recovery (ratio of average total pressure at rake station to tunnel stagnation pressure)
R	Reynolds number (based on a length of 1 foot)

000
100
200
300
400



000 000 000 000 000 000 000 000
000 000 000 000 000 000 000 000
000 000 000 000 000 000 000 000
000 000 000 000 000 000 000 000
000 000 000 000 000 000 000 000

- $\frac{W}{W_{\infty}}$ mass-flow ratio (ratio of mass flow through the induction system to mass flow, at free-stream conditions, through an area equal to the sum of the two inlet areas)
- x/D distance (positive direction downstream) from inlet, along central-body axis, divided by inlet diameter
- α fuselage angle of attack, deg
- δ_c canard-control deflection angle (positive with trailing edge down), deg
- ζ distortion parameter,
$$\left[\frac{p_{t,max} - p_{t,min}}{p_{t,av}} \right]_{rake}$$

Subscripts:

- av average
- max maximum
- min minimum
- nom nominal

APPARATUS AND PROCEDURE

Model Description

The induction-system model had two circular inlets that were located on opposite sides of the fuselage. The diffuser ducts of the system intersected inside the fuselage. A rake of 32 pitot probes was located at the outlet of the induction system approximately 3.2 inches downstream of the intersection. A mass flow meter was connected to a duct that extended downstream from the outlet.

Sketches of the model are shown in figure 1, and photographs are shown in figure 2. The basic fuselage configuration (fuselage 1) was modified by a fairing that extended from the canopy to the tip of the fuselage. The modified fuselage configuration is designated as fuselage 2. Provision was made for mounting a canard control on the fuselage forward of the inlets. The control could be preset at various deflections. In addition, the fuselage was replaced by flat plates (fig. 1(b)).



The sketch in figure 3 shows the internal surface contours of the diffuser. In the supersonic diffuser, the surfaces were conical with semiapex angles of 8.4° and 1.8° , respectively, for the central body and duct. The capture area of each inlet was 5.854 square inches. With the central body in its fully retracted position ($x/D = 0$), the minimum area of 2.3 square inches was located 6.0 inches downstream of the inlet. The area distribution for this central-body position was designed to give the best diffuser performance at a Mach number of 2.50. Area distribution curves for several central-body positions are shown in figure 4.

Boundary-layer air was removed from the internal surfaces through perforations that were vented to the local free stream. The removal systems (B1 to B10) are shown in figure 5.

Apparatus and Test Conditions

The tests were conducted in the low Mach number test section of the Langley Unitary Plan wind tunnel. The test section is 4 feet square and approximately 7 feet long. The tunnel is a variable-pressure, continuous-flow type with an asymmetric sliding-block nozzle for continuous variation of the free-stream Mach number from 1.50 to 2.90.

The tests were conducted at Mach numbers ranging from 1.72 to 2.50. The test Mach numbers were accurate to within ± 0.02 . The stagnation temperature for Mach numbers below 2.30 was 125°F , and for the larger Mach numbers, the stagnation temperature was 150°F .

Internal-flow data were obtained for several tunnel stagnation pressures at a Mach number of 2.50. The maximum pressure recovery for each Reynolds number is presented in figure 6. The jump in pressure recovery between Reynolds numbers of 1.6×10^6 and 2.5×10^6 indicates that the test Reynolds number should be 2.5×10^6 or larger to satisfactorily duplicate the full-scale Reynolds number. Similar trends are expected for the other test Mach numbers. Consequently, the tunnel stagnation pressure was approximately 15 pounds per square inch absolute for all test Mach numbers to insure a Reynolds number larger than 2.5×10^6 . The dew point, measured at stagnation conditions, was maintained below -30°F to assure negligible condensation effects.

Total-pressure recovery was based on the average of 32 pitot pressures that were measured at a station 21.3 inches from the inlets. The arrangement of the pitot probes, which were spaced on an equal-area basis, is sketched in figure 1(c). The distortion parameter was computed by dividing the difference between the largest and smallest pitot pressures by the average pitot pressure. Mass-flow ratio was determined by a calibrated venturi flowmeter connected to the outlet of the induction system.

3

L
1
2
7
2

2

2

•

[REDACTED]

However, the variation of pressure recovery with angle of attack is greater for fuselage 2. The mass-flow ratio and the distortion parameter for the two fuselage models are the same, within estimated accuracy, for angles of attack between 0° and 4° .

For Mach numbers less than 2.50 and $\alpha = 3^\circ$, the internal-flow characteristics for fuselage 1 and the flat-plate model are the same within experimental accuracy. At a Mach number of 2.50, the difference in mass-flow ratios for the flat-plate model and the fuselage models is doubtful. No apparent reason for this difference has been found. The mass-flow ratios for the flat-plate model, with boundary-layer removal system B1, should be less than shown in figure 9. Furthermore, since the flow properties behind the fuselage-bow-shock wave are unknown, it is uncertain whether or not the mass-flow ratios for the flat-plate model should be greater than those for the fuselage models.

A comparison of the results in figure 10 for fuselage 1 shows that adding the canard control with 1.5° deflection did not appreciably alter the internal-flow characteristics of the induction system. Thus, for cruise conditions, the presence of the canard control on the fuselage would not incur any losses in the pressure recovery of the induction system.

Adding the canard control with 5.5° and 9.5° deflection to fuselage 2 resulted in a decrease in pressure recovery of 0.05 and 0.12, respectively, at $\alpha = 3^\circ$. (See fig. 11.) However, for both deflections the loss of pressure recovery with increasing angle of attack was less than the loss for fuselage 2 without the canard ($\alpha > 3^\circ$). Thus, deflection of the canard control would not produce large additional losses in pressure recovery during maneuvers.

SUMMARY OF RESULTS

An investigation to determine the internal-flow characteristics of an induction system with two circular inlets located on opposite sides of an airplane fuselage has been conducted. Supersonic compression was conical and internal. The tests were conducted at Mach numbers ranging from 1.72 to 2.50 and at angles of attack ranging from -4° to 10° . The Reynolds number range was 2.5×10^6 to 4.4×10^6 based on a length of 1 foot. The results obtained are summarized as follows:

1. Boundary-layer removal from the duct was necessary between 0.5 and 1.2 inlet diameters downstream of the inlet in order to approach the desired flow characteristics.

2. At the design Mach number of 2.50, the maximum pressure recovery obtained was 0.76 for the basic fuselage and occurred at an angle of attack of 3° . For the faired-canopy fuselage, the maximum pressure recovery at the design Mach number was 0.80 and occurred at an angle of attack of 1.5° .

3. The mass-flow ratio and distortion parameter were the same for both the basic and faired-canopy fuselages at angles of attack between 0° and 4° .

4. The addition of a canard control with a deflection angle of 1.5° had no appreciable effect on the internal-flow characteristics of the induction system (basic fuselage). At deflection angles of 5.5° and 9.5° (faired-canopy fuselage), a loss in pressure recovery occurred; however, the loss of pressure recovery with increasing angle of attack was less than that for the same fuselage without the canard for angles of attack greater than 3° .

Langley Research Center,
National Aeronautics and Space Administration,
Langley Field, Va., December 14, 1960.

REFERENCES

1. Davis, Wallace F., and Scherrer, Richard: Aerodynamic Principles for the Design of Jet-Engine Induction Systems. NACA RM A55F16, 1956.
2. Bowditch, David N., and Anderson, Bernhard H.: Performance of an Isentropic, All-Internal-Contraction, Axisymmetric Inlet Designed for Mach 2.50. NACA RM E58E16, 1958.
3. Pfyl, Frank A., and Watson, Earl C.: An Experimental Investigation of Circular Internal-Compression Inlets With Translating Centerbodies Employing Boundary-Layer Removal at Mach Numbers From 0.85 to 3.50. NASA MEMO 2-19-59A, 1959.
4. Martin, Norman J.: Exploratory Investigation of the Effects of Boundary-Layer Control on the Pressure-Recovery Characteristics of a Circular Internal-Contraction Inlet With Translating Centerbody at Mach Numbers of 2.00 and 2.35. NASA MEMO 12-31-58A, 1959.
5. Oehman, Waldo I., and Vahl, Walter A.: Tests of a Fixed-Geometry External-Compression Induction-System Model, Alone and in Combination With a Missile Forebody Configuration at Mach Numbers Between 2.20 and 2.86. NASA TM X-307, 1961.

TABLE I.- INTERNAL-FLOW CHARACTERISTICS OF AN INDUCTION SYSTEM HAVING
TWO CIRCULAR INTERNAL-COMPRESSION INLETS

(a) Inlets with fuselage 1

Mach number, M	Angle of attack, α , deg	Central-body-tip position, x/D (a)	Peak pressure recovery, ($P_{t,r}$) _{peak}	Mass-flow ratio, w/w_∞	Distortion parameter, ξ
Boundary-layer removal system B1; canard control removed					
1.80	3.1	1.76	0.8818	0.6742	0.0751
2.00	-3.2	1.71	.7807	.6857	.0696
2.00	0	1.63	.8271	.7272	.1094
2.00	3.1	1.56	.8512	.7218	.0789
2.20	-3.2	1.57	.7069	.7381	.1474
2.20	-3.2	1.62	.7041	.7195	.1048
2.20	0	1.30	.8102	.7953	.0965
2.20	3.1	1.13	.8420	.8264	.0673
2.20	3.1	1.17	.8370	.8245	.0634
2.50	-3.2	.74	.6295	.8730	.1149
2.50	-3.2	.78	.6493	.8770	.0967
2.50	-3.2	.81	.6602	.8679	.0827
2.50	-3.2	.85	.6537	.8625	.0815
2.50	0	.46	.7449	.8747	.0810
2.50	0	.50	.7443	.8758	.0779
2.50	3.1	.46	.7602	.8950	.0880
2.50	3.1	.49	.7574	.8822	.0855
2.50	6.3	.76	.7206	.8996	.0609
2.50	6.3	.80	.7290	.9051	.0638
Boundary-layer removal system B4; canard control removed					
2.50	3.1	0.55	0.7601	0.9134	0.0676
2.50	3.1	.60	.7586	.9101	.0591
2.50	3.1	.66	.7570	.9051	.0494
Boundary-layer removal system B5; canard control removed					
2.50	0	0.43	0.7400	0.8640	0.0820
2.50	0	.49	.7481	.8478	.0720
2.50	1.6	.57	.7492	.8854	.0899
2.50	1.6	.42	.7678	.8712	.0803
2.50	1.6	.49	.7620	.8471	.0753
2.50	3.1	.43	.7704	.8776	.0750
2.50	3.1	.49	.7669	.8600	.0730
2.50	3.1	.62	.7591	.8521	.0498
Boundary-layer removal system B6; canard control removed					
2.20	0	1.38	0.7951	0.7959	0.0889
2.20	0	1.44	.7740	.7899	.1046
2.20	3.1	1.41	.7699	.7982	.0716
2.50	0	.52	.7329	.8817	.0864
2.50	0	.60	.7437	.8668	.0653
2.50	1.5	.43	.7640	.8805	.0772
2.50	1.5	.50	.7560	.8906	.0762
2.50	3.1	.35	.7372	.9029	.1131
2.50	3.1	.44	.7593	.8909	.0893
2.50	3.1	.53	.7694	.8873	.0728
2.50	3.1	.62	.7652	.8730	.0507

^a Inlet diameters upstream of the inlet plane.

L-1270

TABLE I.- INTERNAL-FLOW CHARACTERISTICS OF AN INDUCTION SYSTEM HAVING
TWO CIRCULAR INTERNAL-COMPRESSION INLETS - Continued

(a) Inlets with fuselage 1 - Concluded

Mach number, M	Angle of attack, α , deg	Central-body-tip position, x/D (a)	Peak pressure recovery, $(P_{t,r})_{peak}$	Mass-flow ratio, w/w_∞	Distortion parameter, ξ
Boundary-layer removal system B7; canard control removed					
2.44	3.1	1.44	0.6464	0.8246	0.0976
Boundary-layer removal system B8; canard control removed					
2.44	3.2	1.45	0.6551	0.8594	0.0880
2.44	3.2	1.51	.6407	.8376	.0871
Boundary-layer removal system B9; canard control removed					
2.35	3.1	1.48	0.6084	0.8466	0.1327
2.35	3.1	1.57	.6695	.7885	.1068
2.35	3.1	1.66	.6432	.7670	.0991
Boundary-layer removal system B1; canard control deflected 1.5°					
1.80	3.1	1.74	0.8860	0.6779	0.0761
1.80	3.1	1.77	.8817	.6612	.0558
1.80	3.1	1.79	.8724	.6532	.0614
2.00	3.1	1.57	.8580	.7088	.0647
2.00	3.1	1.60	.8480	.7040	.0579
2.00	3.1	1.63	.8378	.7045	.0689
2.20	3.1	1.15	.7370	.8545	.0908
2.20	3.1	1.17	.8326	.8159	.0954
2.20	3.1	1.21	.8243	.8094	.0912
2.50	-3.2	.77	.6732	.8704	.0769
2.50	-3.2	.81	.6710	.8594	.0740
2.50	-3.2	.85	.6639	.8593	.0811
2.50	0	.50	.7396	.8790	.0797
2.50	0	.55	.7461	.8694	.0784
2.50	0	.61	.7430	.8644	.0715
2.50	1.5	.46	.7506	.8924	.0904
2.50	1.5	.51	.7652	.8759	.0696
2.50	1.5	.56	.7536	.8750	.0769
2.50	3.1	.48	.7652	.8963	.0883
2.50	3.1	.53	.7575	.8983	.0892
2.50	3.1	.58	.7602	.8807	.0782
2.50	6.2	.79	.7290	.8690	.0693
2.50	6.2	.84	.7268	.8720	.0690
2.50	6.2	.89	.7210	.8574	.0718
Boundary-layer removal system B1; canard control deflected 9.5°					
1.80	3.1	1.78	0.8647	0.6866	0.0614
1.80	3.1	1.81	.8606	.6574	.0555
2.00	3.1	1.65	.8045	.7345	.0889
2.00	3.1	1.67	.7993	.7242	.1062
2.20	3.1	1.40	.7597	.8013	.1065
2.20	3.1	1.43	.7592	.7859	.0985
2.20	3.1	1.45	.7467	.7876	.0987

^aInlet diameters upstream of the inlet plane.

TABLE I.- INTERNAL-FLOW CHARACTERISTICS OF AN INDUCTION SYSTEM HAVING
TWO CIRCULAR INTERNAL-COMPRESSION INLETS - Continued

(b) Inlets with fuselage 2

Mach number, M	Angle of attack, α , deg	Central-body-tip position, x/D (a)	Peak pressure recovery, $(P_{t,r})_{peak}$	Mass-flow ratio, w/w_∞	Distortion parameter, ξ
Boundary-layer removal system B1; canard control removed					
2.50	-3.2	1.50	0.5936	0.7828	0.2134
2.50	-3.2	1.52	.5893	.7760	.2067
2.50	0	.64	.5260	.9148	.3311
2.50	0	.68	.7598	.8986	.0852
2.50	1.6	.48	.7989	.8945	.0775
2.50	1.6	.50	.7961	.8920	.0794
2.50	1.6	1.20	.7060	.8225	.0589
2.50	3.1	.49	.7751	.9081	.0966
2.50	3.1	.52	.7906	.9050	.0790
2.50	3.1	1.23	.7052	.8159	.0441
2.50	6.2	.71	.6266	.9073	.1556
2.50	6.2	.75	.7009	.8945	.1355
Boundary-layer removal system B2; canard control removed					
2.50	0	0.68	0.7510	0.8989	0.0848
2.50	1.5	.62	.7458	.9207	.0893
2.50	3.1	.58	.7826	.9065	.0685
2.50	3.1	.60	.7856	.8923	.0640
2.50	3.1	.63	.7826	.9008	.0638
Boundary-layer removal system B3; canard control removed					
2.00	3.1	1.58	0.7927	0.8035	0.1252
2.00	3.1	1.61	.8512	.7581	.0761
2.20	3.1	1.18	.8531	.8670	.0880
2.20	3.1	1.18	.8109	.8853	.0501
2.20	3.1	1.21	.8429	.8705	.0936
2.20	3.1	1.23	.8439	.8532	.0794
Boundary-layer removal system B5; canard control removed					
2.00	3.1	1.55	0.8731	0.7334	0.0626
2.00	3.1	1.58	.8653	.7289	.0621
2.20	3.1	1.35	.8061	.8136	.0512
2.20	3.1	1.40	.8114	.7815	.0563
2.50	3.1	.45	.7909	.9169	.0641
2.50	3.1	.49	.7903	.9164	.0583
2.50	3.1	.55	.7919	.9064	.0516
Boundary-layer removal system B10; canard control removed					
1.72	3.1	1.87	0.8899	0.6817	0.1287
1.91	3.1	1.72	.8782	.7184	.1173
2.11	3.1	1.53	.8180	.7807	.1210
2.35	-3.1	1.63	.6593	.7772	.2374
2.35	0	1.40	.7488	.8342	.0987
2.35	1.6	1.39	.7618	.8432	.0804
2.35	3.1	1.39	.7732	.8227	.0638
2.35	3.1	1.47	.7404	.8064	.0696
2.35	6.2	1.58	.6745	.7653	.1583

^aInlet diameters upstream of the inlet plane.

L-1270

TABLE I.- INTERNAL-FLOW CHARACTERISTICS OF AN INDUCTION SYSTEM HAVING
TWO CIRCULAR INTERNAL-COMPRESSION INLETS - Continued

(b) Inlets with fuselage 2 - Concluded

Mach number, M	Angle of attack, α , deg	Central-body-tip position, x/D (a)	Peak pressure recovery, $(P_{t,r})_{\text{peak}}$	Mass-flow ratio, w/w_∞	Distortion parameter, ξ
Boundary-layer removal system B1; canard control deflected 5.5°					
1.80	3.1	1.76	0.8884	0.6830	0.0704
1.80	3.1	1.80	.8759	.6777	.0606
2.00	3.1	1.60	.8412	.7368	.0845
2.00	3.1	1.60	.8420	.7395	.0823
2.00	3.1	1.63	.8213	.7260	.0862
2.20	-3.1	1.54	.6573	.7342	.0596
2.20	-3.1	1.57	.6926	.7324	.1556
2.20	0	1.50	.7486	.7623	.1575
2.20	0	1.52	.7470	.7467	.1527
2.20	1.5	1.29	.8107	.8160	.1140
2.20	1.5	1.32	.8082	.8065	.1102
2.20	3.1	1.24	.8194	.8123	.1062
2.20	3.1	1.27	.8178	.8114	.0909
2.20	3.1	1.28	.8180	.7993	.0960
2.20	6.2	1.42	.7387	.7888	.1161
2.20	6.2	1.45	.7483	.7544	.1400
2.20	6.2	1.48	.7416	.7490	.1452
2.20	9.4	1.56	.6682	.7232	.1647
2.20	9.4	1.60	.6694	.6940	.1569
2.50	-3.1	.80	.5820	.8549	.1272
2.50	-3.1	.84	.6191	.8609	.0988
2.50	-3.1	1.30	.5767	.8041	.2707
2.50	0	.59	.6579	.8771	.1076
2.50	0	.63	.6573	.8710	.1071
2.50	0	.65	.6637	.8784	.0984
2.50	0	1.35	.6116	.7945	.1468
2.50	1.5	.54	.6463	.8874	.1375
2.50	1.5	.57	.7233	.8890	.0796
2.50	1.5	.61	.7164	.8944	.0807
2.50	3.1	.65	.7380	.8867	.0873
2.50	3.1	.67	.7391	.8804	.0822
2.50	3.1	.70	.7367	.8695	.0767
2.50	6.2	.74	.7085	.9165	.0974
2.50	6.2	.79	.7250	.9058	.0663
2.50	9.4	.91	.5349	.8865	.1723
2.50	9.4	.96	.6409	.8751	.0544
2.50	9.4	.99	.6632	.8758	.0613
Boundary-layer removal system B1; canard control deflected 9.5°					
2.50	-3.1	0.85	0.5165	0.8178	0.1951
2.50	-3.1	.91	.5303	.8180	.1149
2.50	-3.1	.95	.5420	.8188	.0962
2.50	-3.1	1.01	.5535	.8221	.0812
2.50	0	.85	.5636	.8385	.1383
2.50	0	.88	.5774	.8332	.1286
2.50	0	.92	.5751	.8405	.1350
2.50	0	.96	.6051	.8417	.1025
2.50	1.6	.71	.5829	.8577	.1593
2.50	1.6	.77	.6148	.8643	.1280
2.50	1.6	.82	.6087	.8672	.1243
2.50	3.1	.71	.6646	.8814	.1097
2.50	3.1	.75	.6675	.8804	.1005
2.50	3.1	.79	.6775	.8807	.0784
2.50	3.1	.83	.6693	.8805	.0793
2.50	6.2	.90	.6832	.9025	.0548

^a Inlet diameters upstream of the inlet plane.

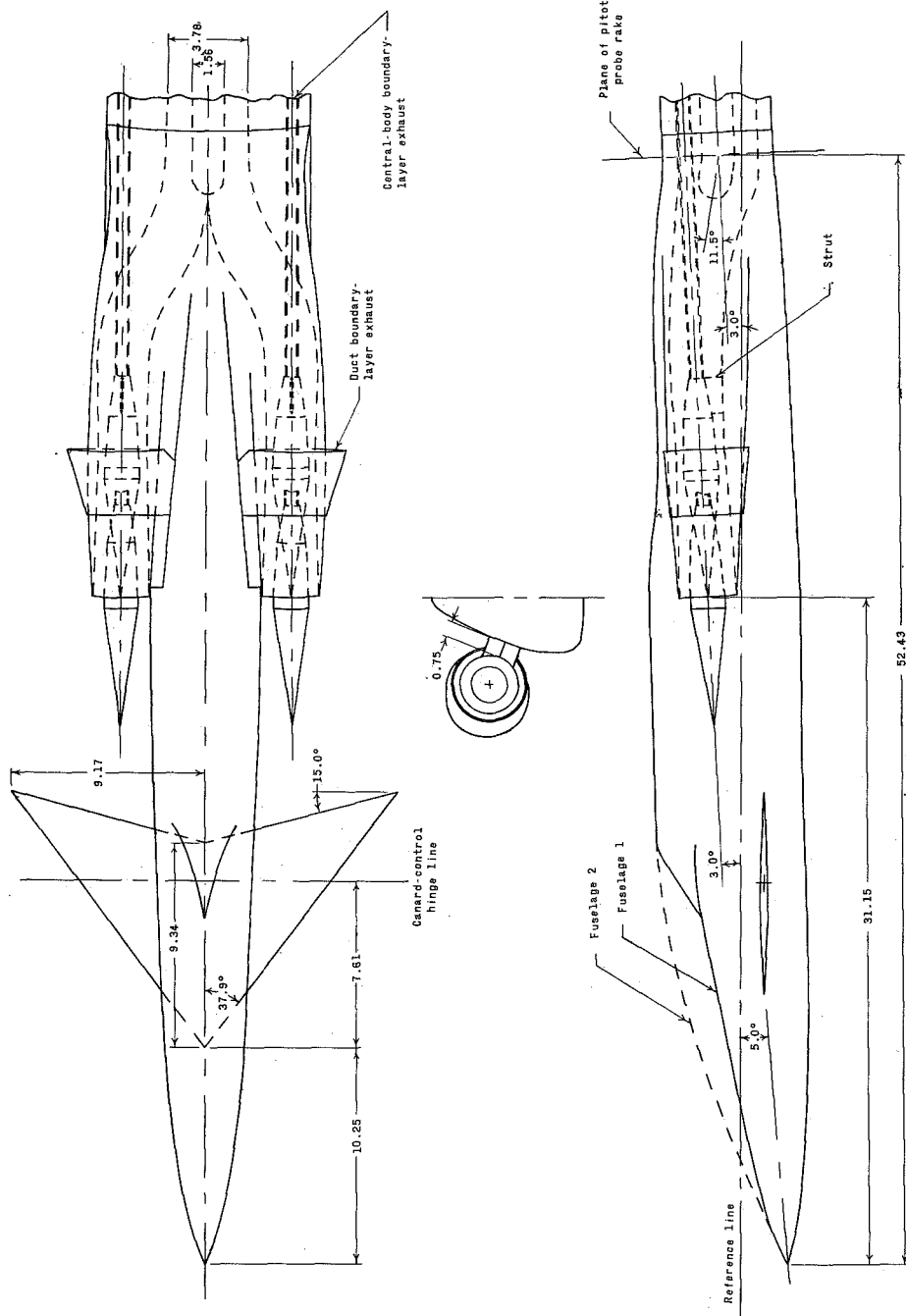
TABLE I.- INTERNAL-FLOW CHARACTERISTICS OF AN INDUCTION SYSTEM HAVING
TWO CIRCULAR INTERNAL-COMPRESSION INLETS - Concluded

(c) Inlets with flat plates; boundary-layer removal system B1

Mach number, M	Angle of attack, α , deg	Central-body-tip position, x/D (a)	Peak pressure recovery, ($P_{t,r}$) _{peak}	Mass-flow ratio, w/w_∞	Distortion parameter, ξ
1.80	0	1.82	0.8683	0.7130	0.1307
1.80	3.1	1.81	.8894	.6937	.0844
1.80	3.1	1.84	.8857	.6785	.0817
2.00	3.1	1.67	.8574	.7651	.0855
2.00	3.1	1.72	.8447	.7481	.0927
2.20	3.1	1.45	.7986	.8779	.1075
2.20	3.1	1.47	.8303	.8312	.0882
2.20	3.1	1.50	.8252	.8243	.0840
2.50	0	.80	.8137	.9879	.0645
2.50	0	.83	.8069	.9913	.0658
2.50	1.6	.84	.8119	.9913	.0597
2.50	3.1	.84	.7998	1.0079	.0742
2.50	3.1	.87	.8143	.9864	.0502
2.50	3.1	.91	.8068	.9891	.0530

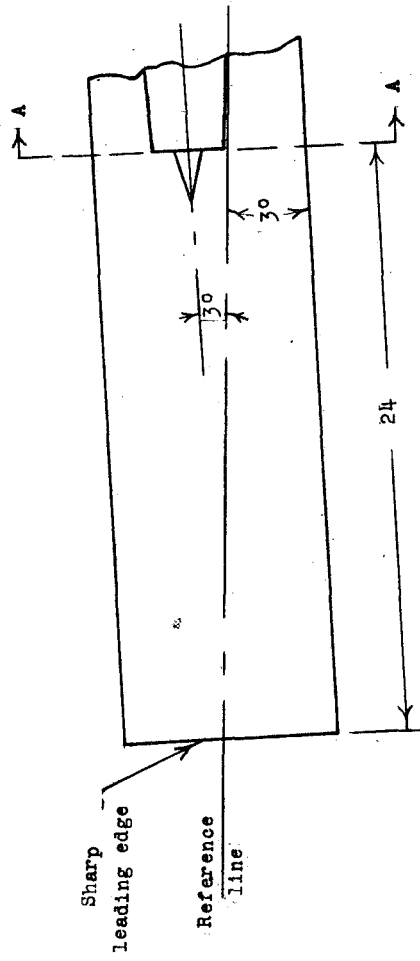
^aInlet diameters upstream of the inlet plane.

L
1
2
7
0



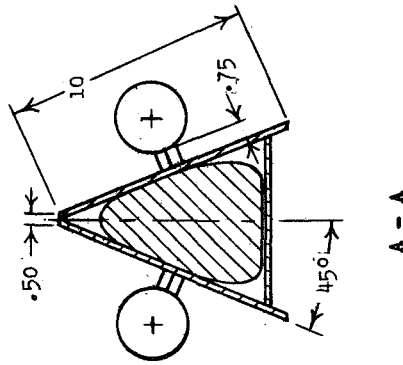
(a) Fuselage 1 and fuselage 2.

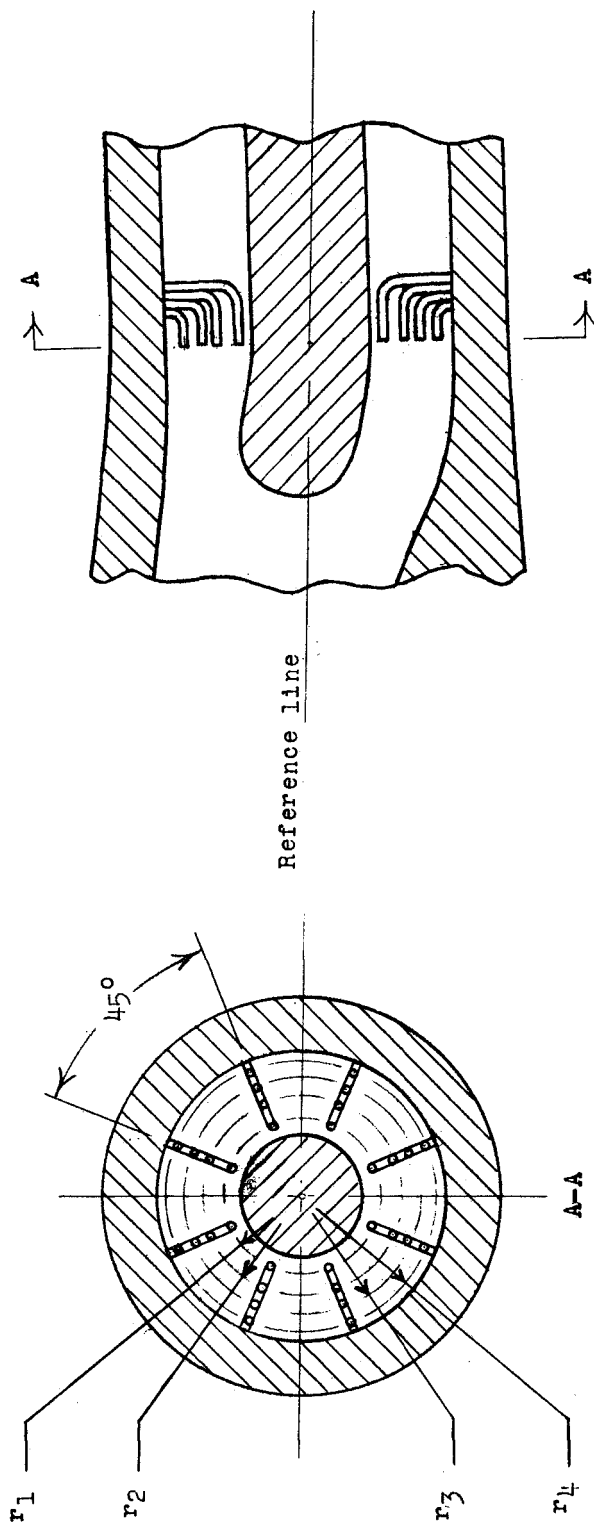
Figure 1.- Sketches of the induction-system model. (All dimensions are in inches unless otherwise noted.)



(b) Flat-plate model.

Figure 1.- Continued.

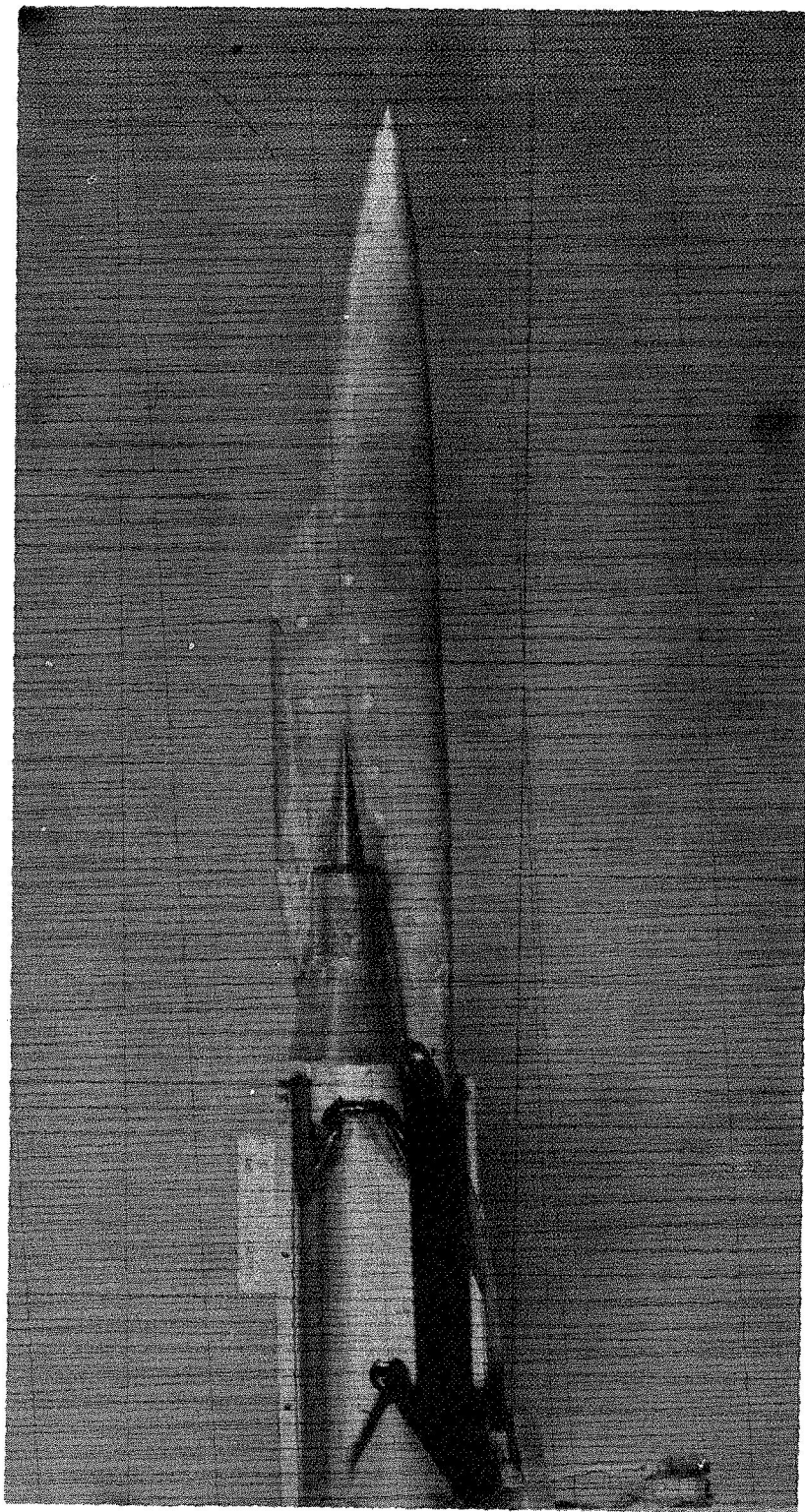




$r_1 = 0.99$
 $r_2 = 1.31$
 $r_3 = 1.57$
 $r_4 = 1.79$

(c) Pitot-probe rake.

Figure 1.- Concluded.

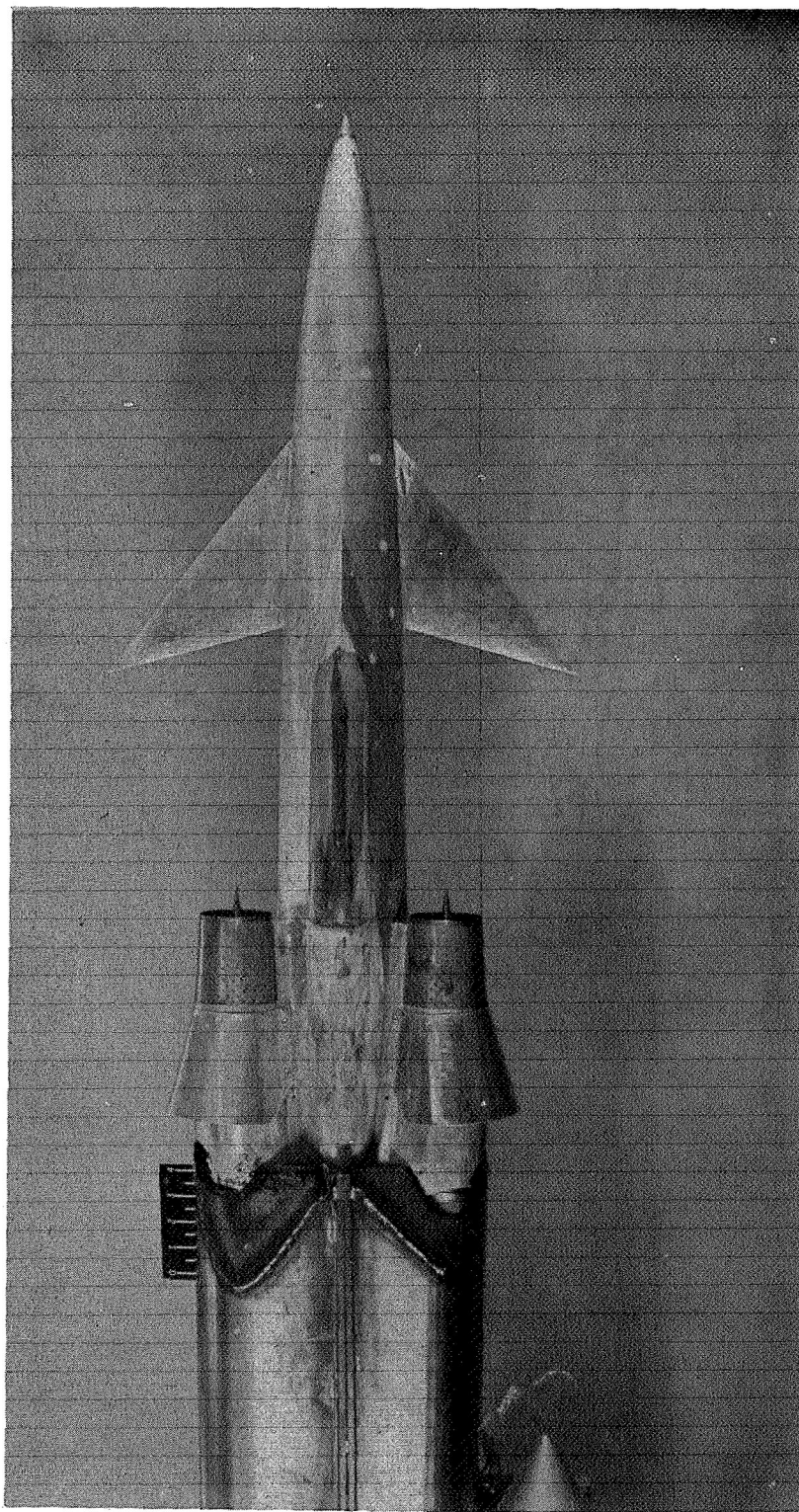


(a) Fuselage 1.

Figure 2.- Model photographs.

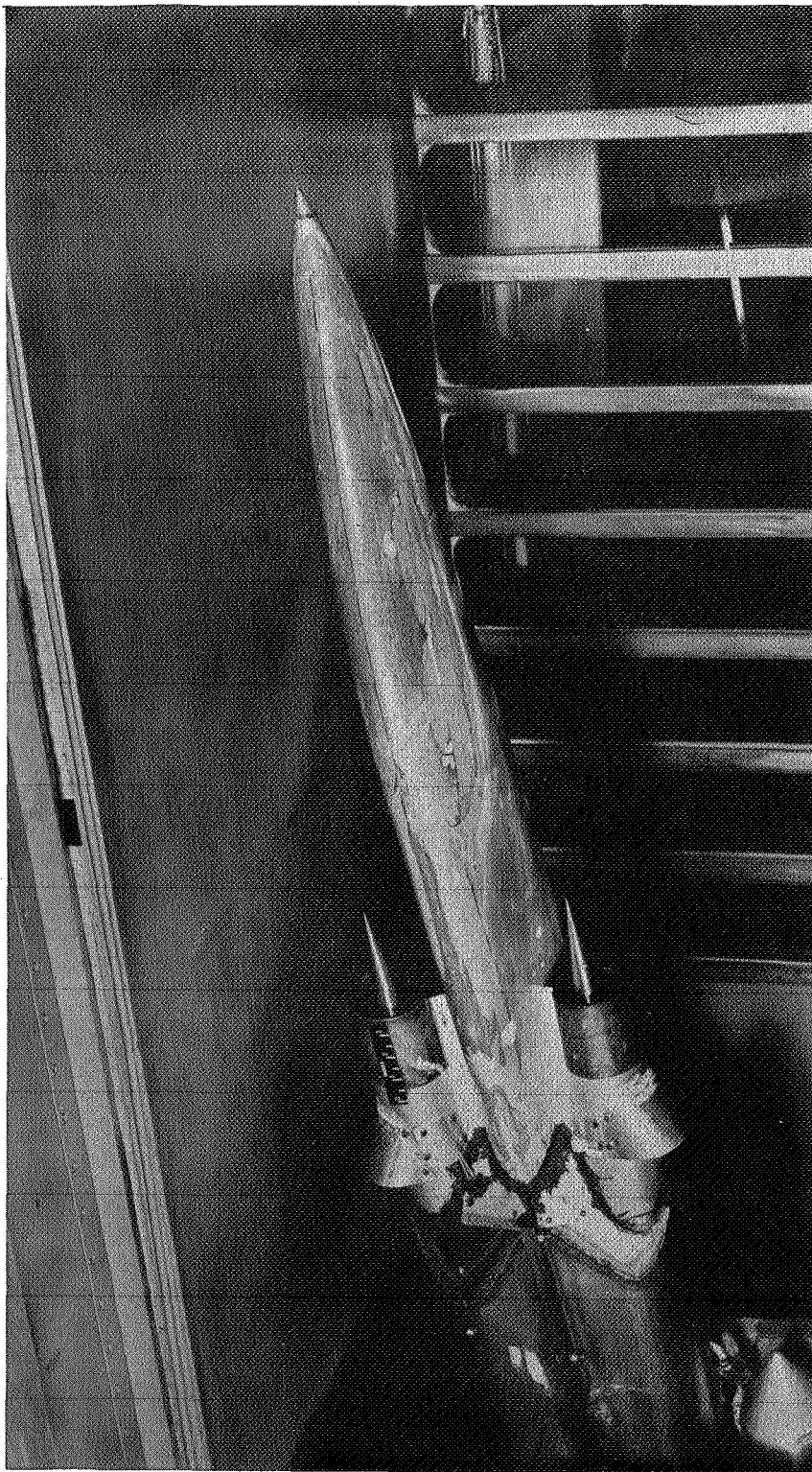
L-57-5015

L-1270



(b) Fuselage 1 with canard control. L-57-5011

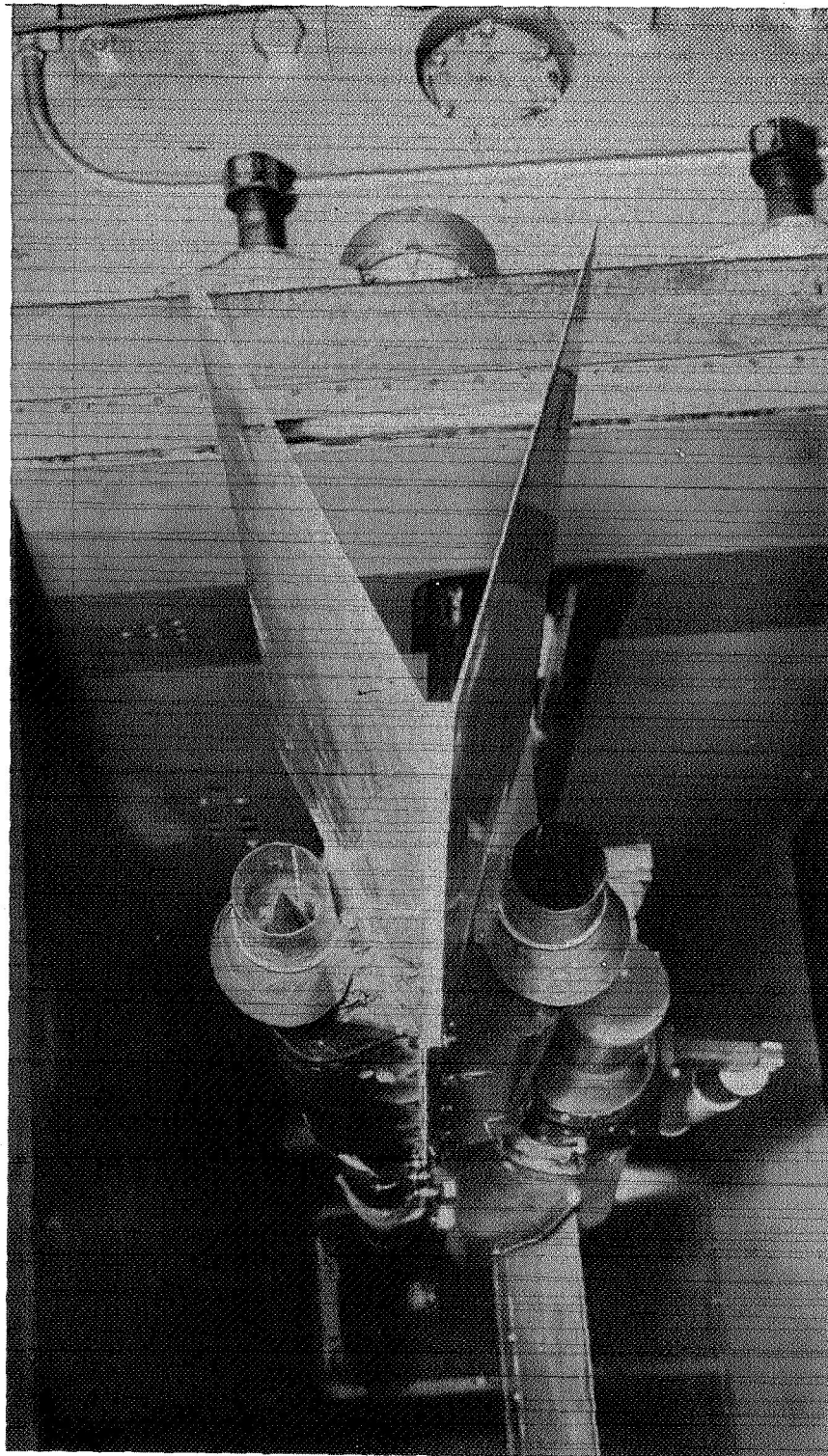
Figure 2.- Continued.



(c) Fuselage 2.

I-57-4872

Figure 2.- Continued.



(d) Flat-plate model.

L-57-4968

Figure 2.- Concluded.

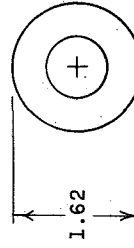
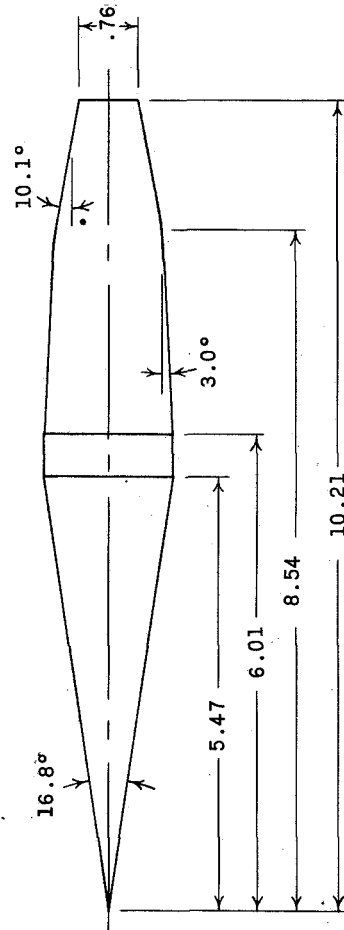
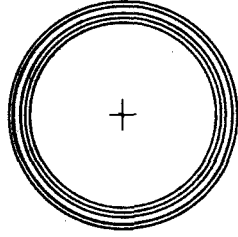
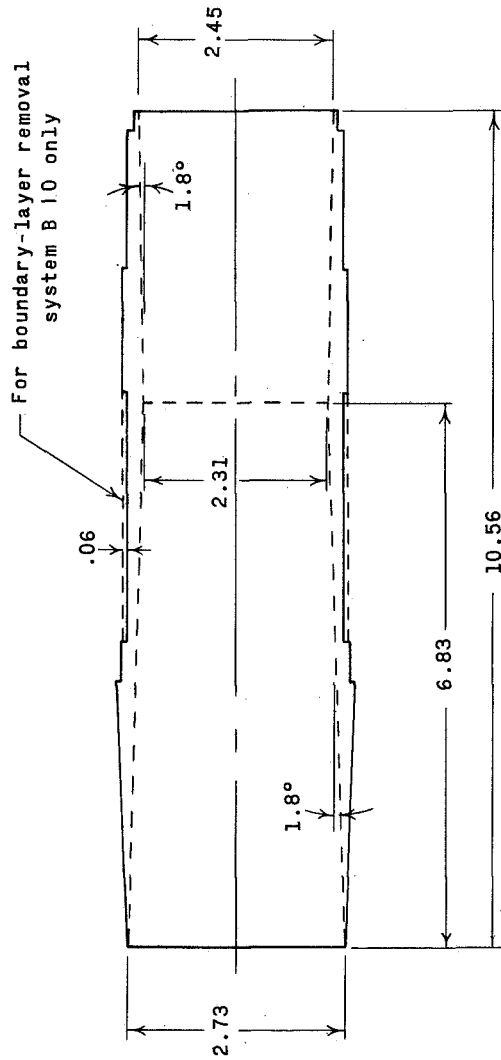


Figure 3.- Duct and central-body details. (All dimensions are in inches unless otherwise noted.)

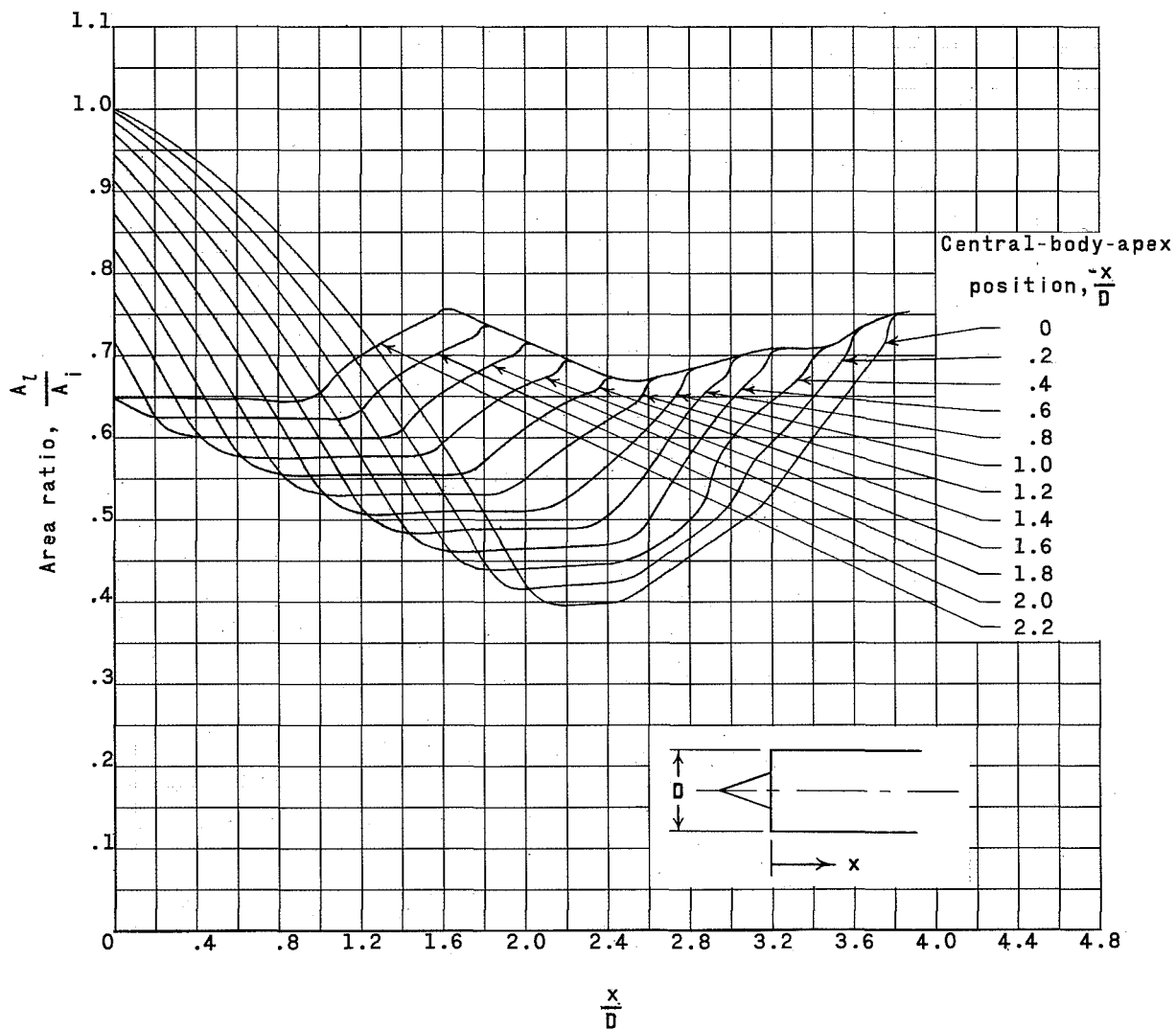
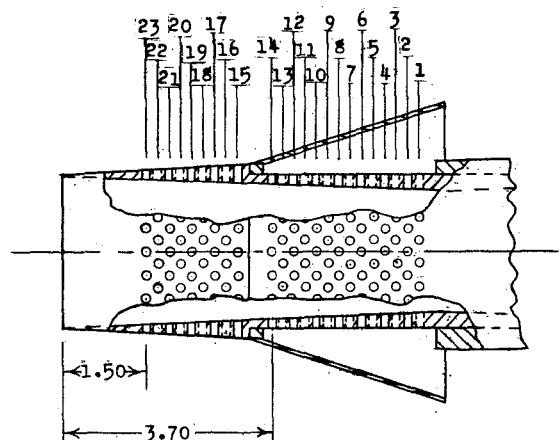


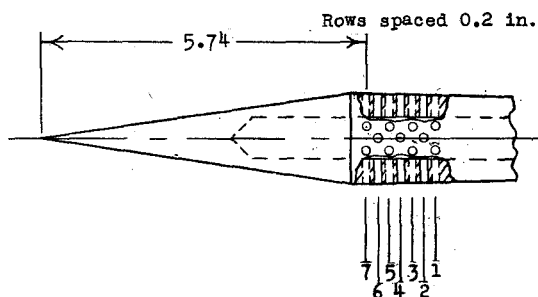
Figure 4.- Annular-area distribution.



24 equally spaced holes per row in duct wall and central body, 0.052-inch diameter



Rows spaced 0.2 inch except between rows 14 and 15



Boundary-layer removal system	Duct-wall rows open	Central-body rows open
B 1	4, 5, 7 through 23	All
B 2	4 through 10, 12, 14, 15, 17, 19, 20	All
B 3	1, 3, 5, 7, 9, 11, 13, 15 through 23	All
B 4	1, 3, 5, 7, 9, 11, 13, 15, 17, 19	All
B 5	1 through 20	All
B 6	7 through 20	All
B 7	1 through 9	All
B 8	None	All
B 9	6 through 14	All
B 10	1 through 9	All

Duct wall in region of rows 1 through 9 is 0.06-inch thicker for B 10 than for all other boundary-layer removal systems.

Figure 5.- Boundary-layer removal systems. (All dimensions are in inches unless otherwise noted.)

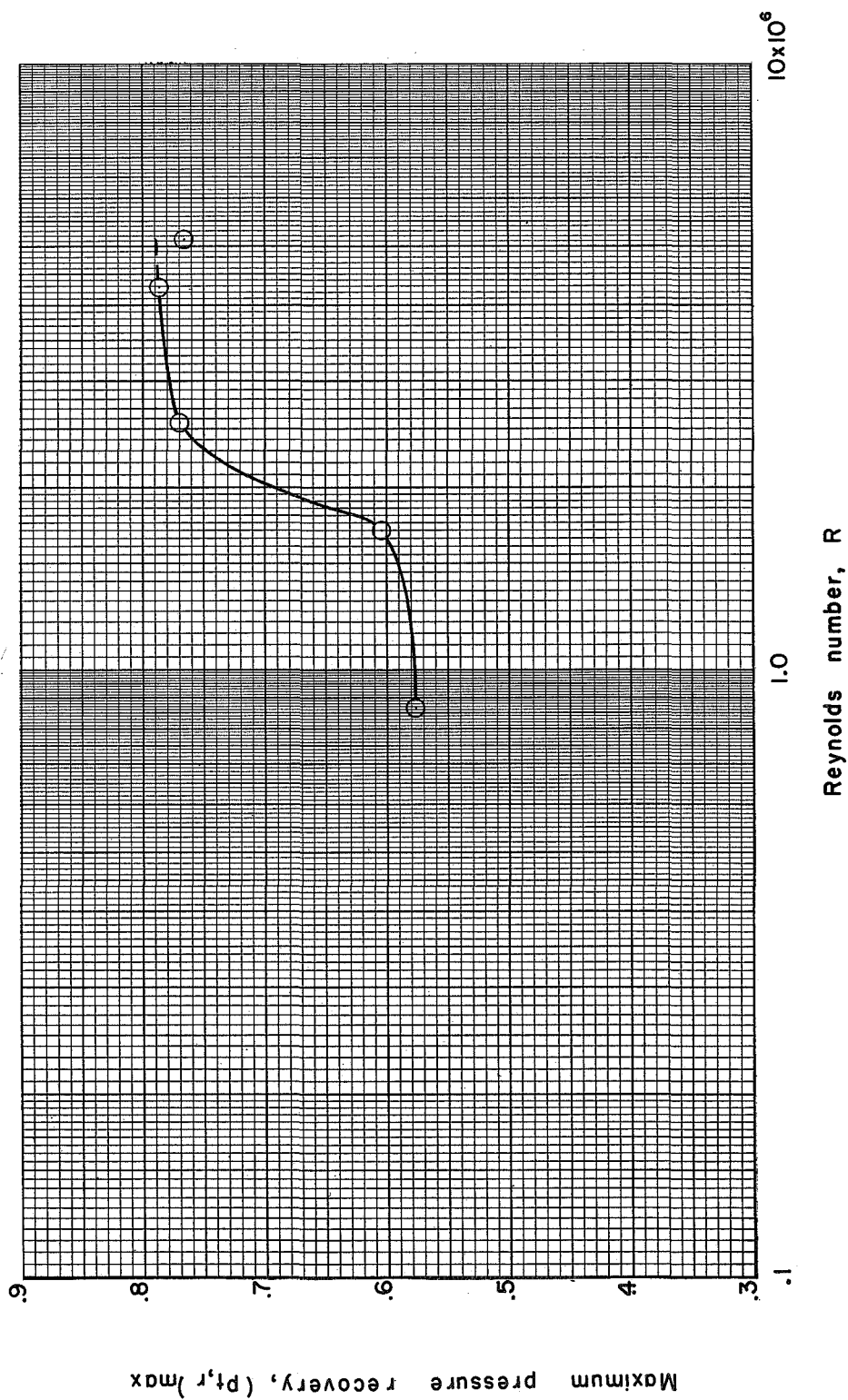
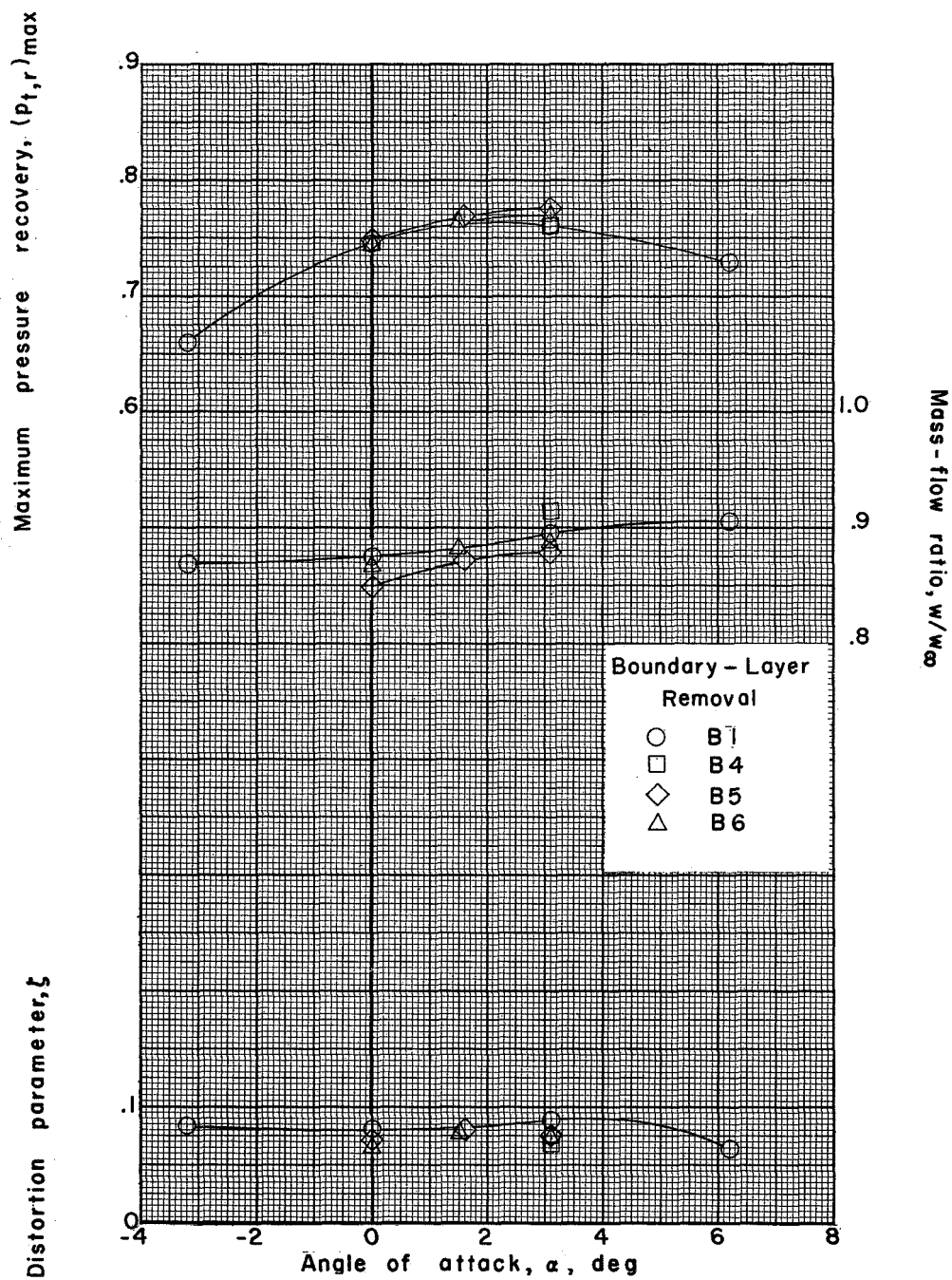
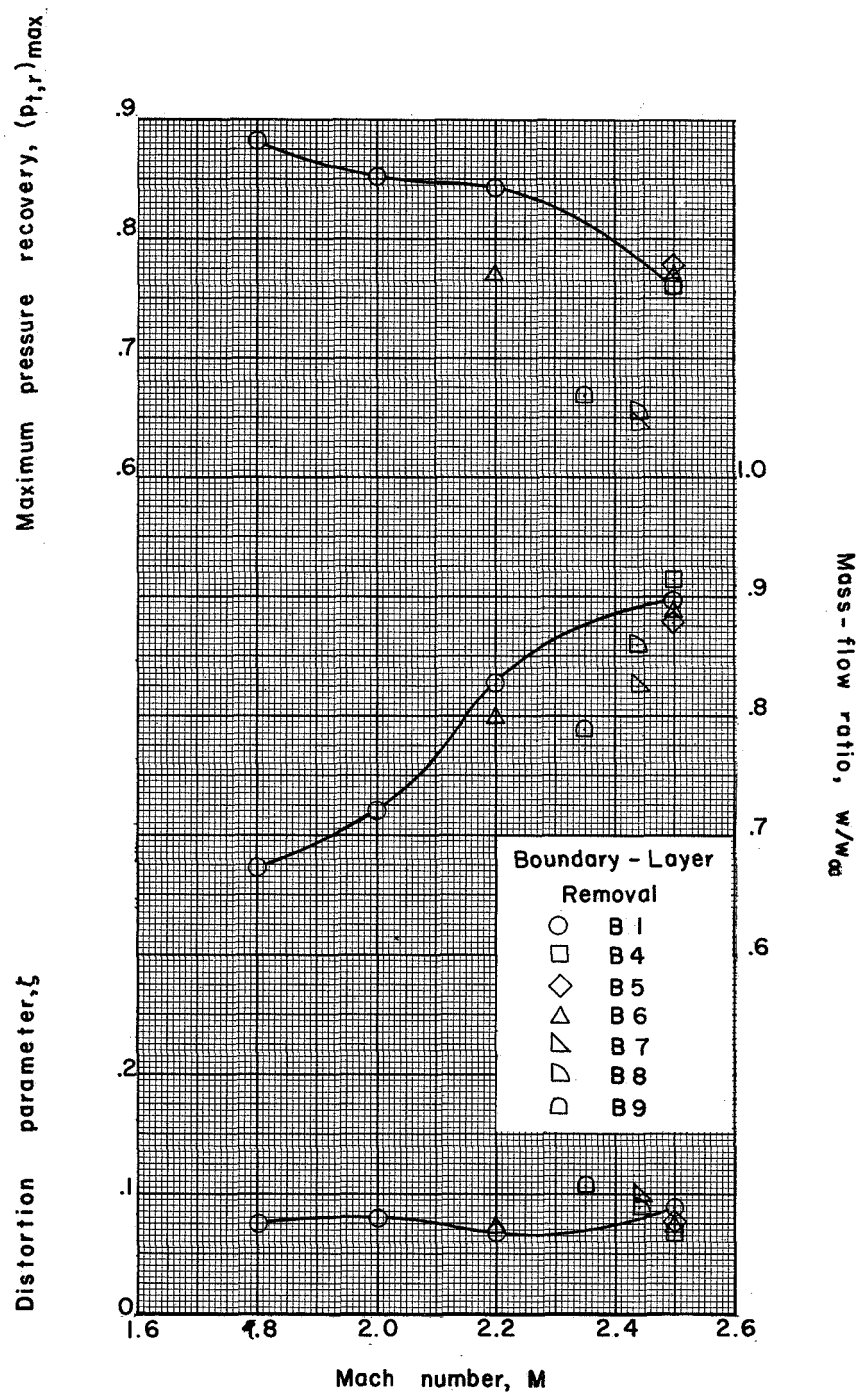


Figure 6.- Effect of Reynolds number on maximum pressure recovery. Fuselage 1 with boundary-layer removal system B1; $M = 2.50$.



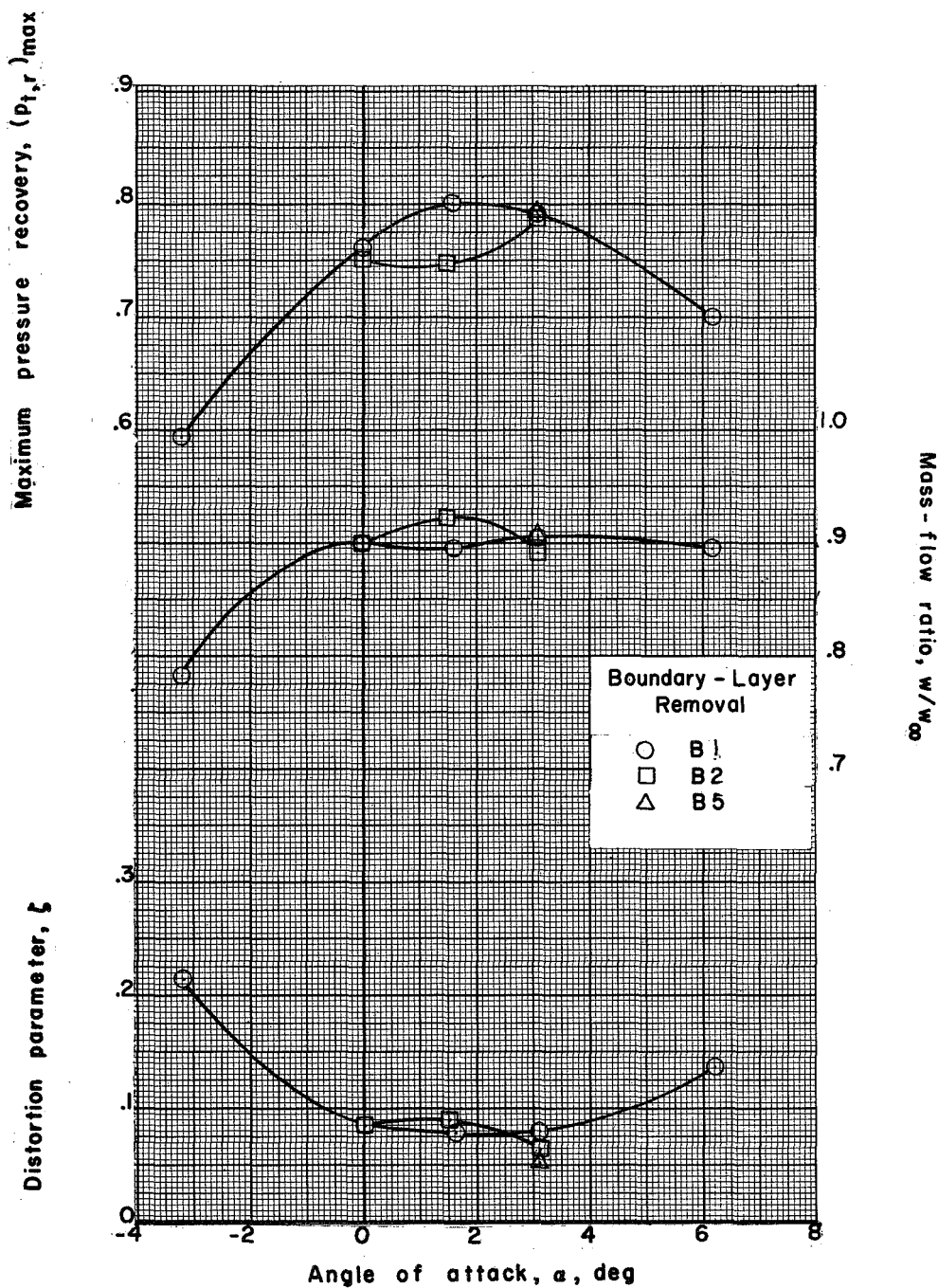
(a) Effect of angle of attack. $M = 2.50$.

Figure 7.- Internal-flow characteristics of the induction system for several boundary-layer removal systems. Fuselage 1.



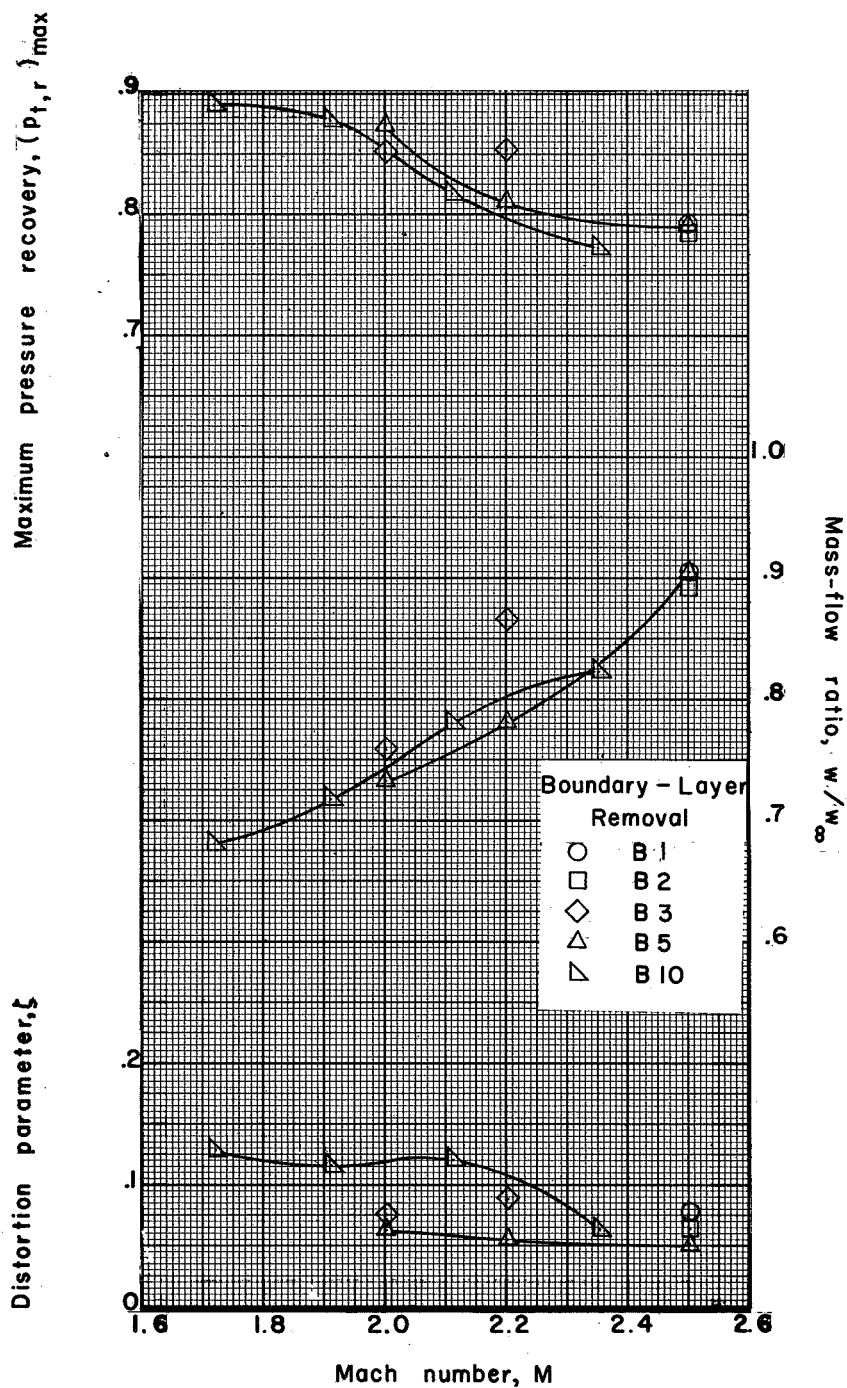
(b) Effect of Mach number. $\alpha_{nom} = 3^\circ$.

Figure 7.- Concluded.



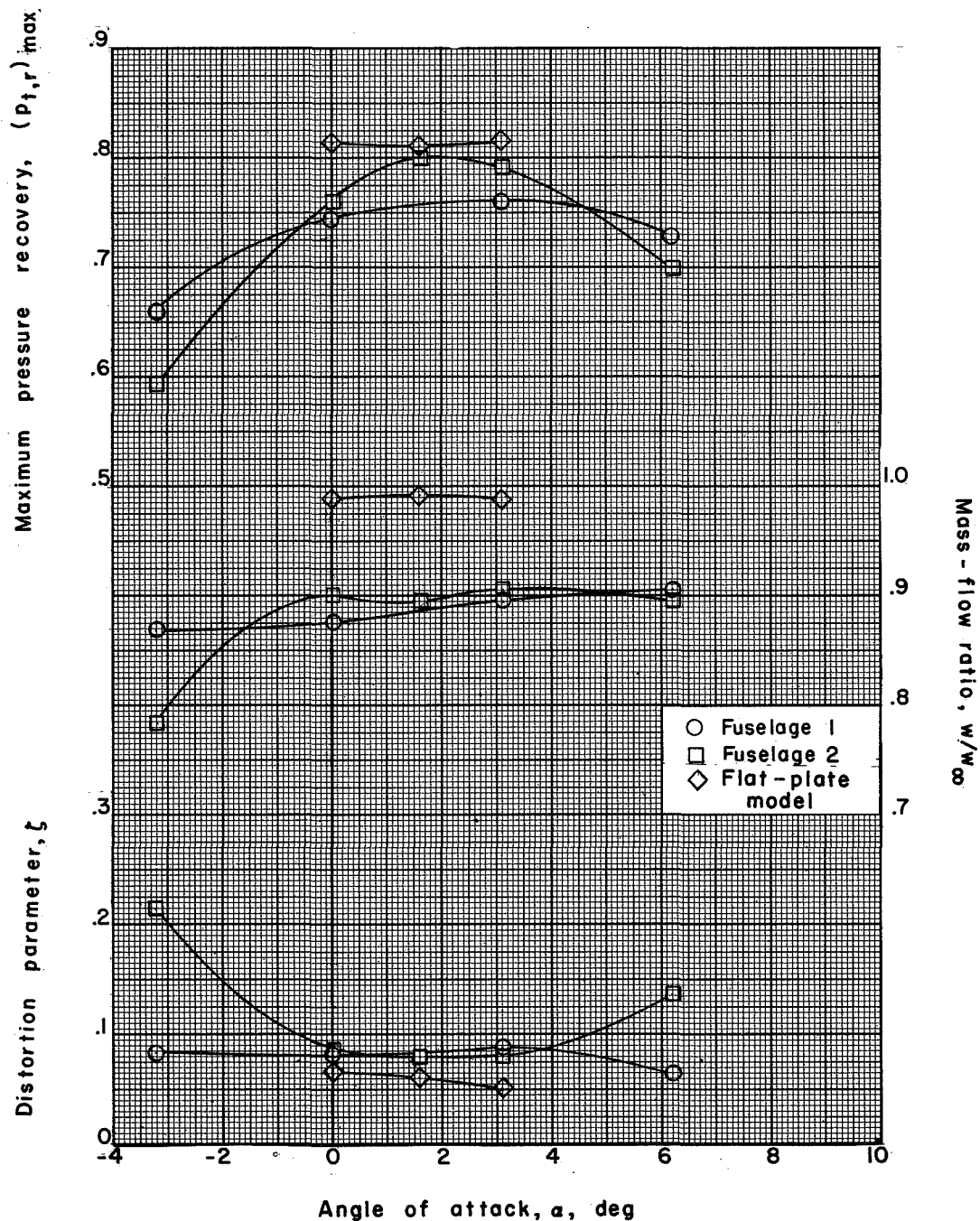
(a) Effect of angle of attack. $M = 2.50$.

Figure 8.- Internal-flow characteristics of the induction system for several boundary-layer removal systems. Fuselage 2.



(b) Effect of Mach number. $\alpha_{\text{nom}} = 3^\circ$.

Figure 8.- Concluded.



(a) Effect of angle of attack. $M = 2.50$.

Figure 9.- Comparison of induction-system internal-flow characteristics for fuselage 1, fuselage 2, and the flat-plate model. Boundary-layer removal system B1.

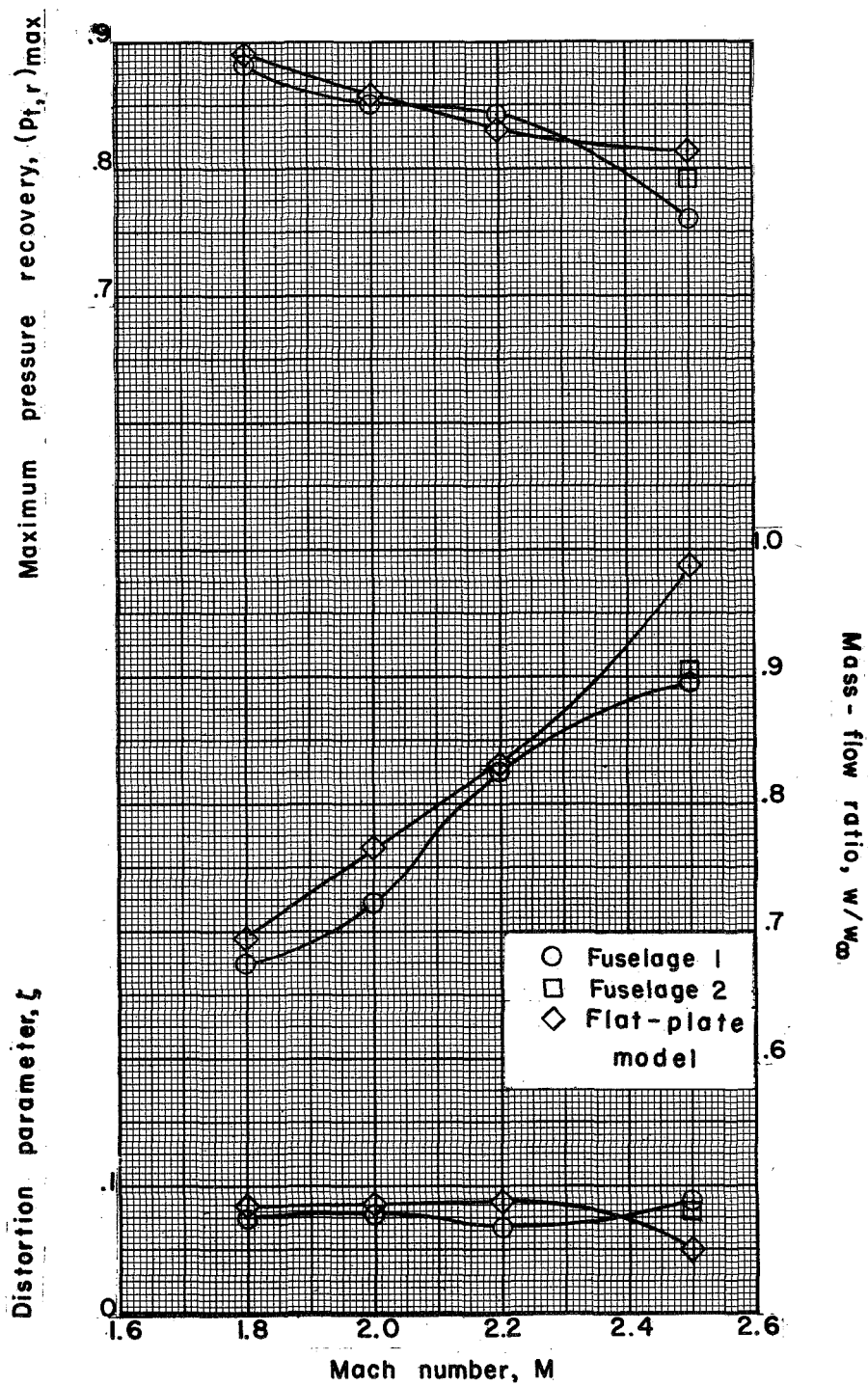
(b) Effect of Mach number. $\alpha_{nom} = 3^\circ$.

Figure 9.- Concluded.

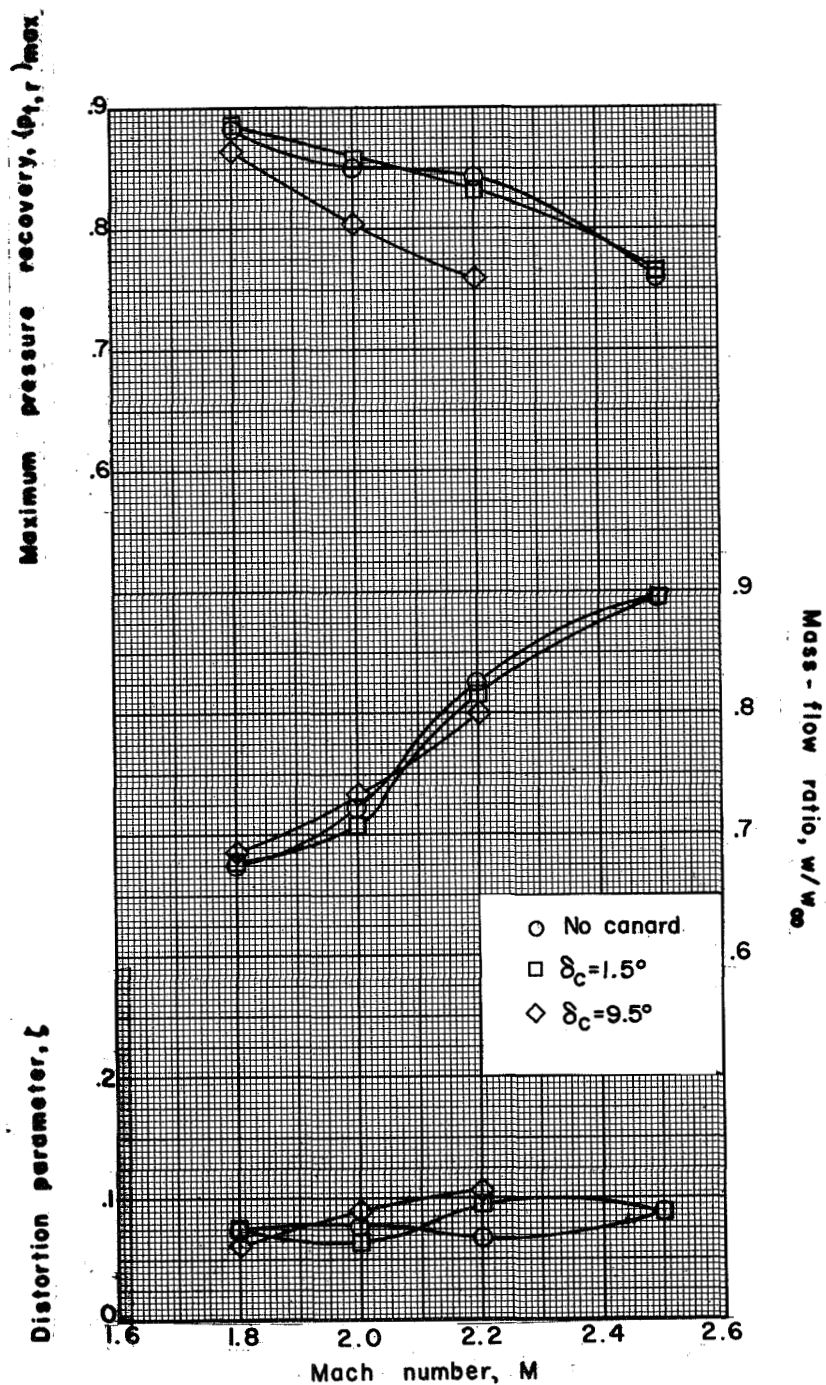


Figure 10.- Effect of canard and canard-control deflection on the induction-system internal-flow characteristics for fuselage 1. Boundary-layer removal system B1; $\alpha_{nom} = 30^\circ$.

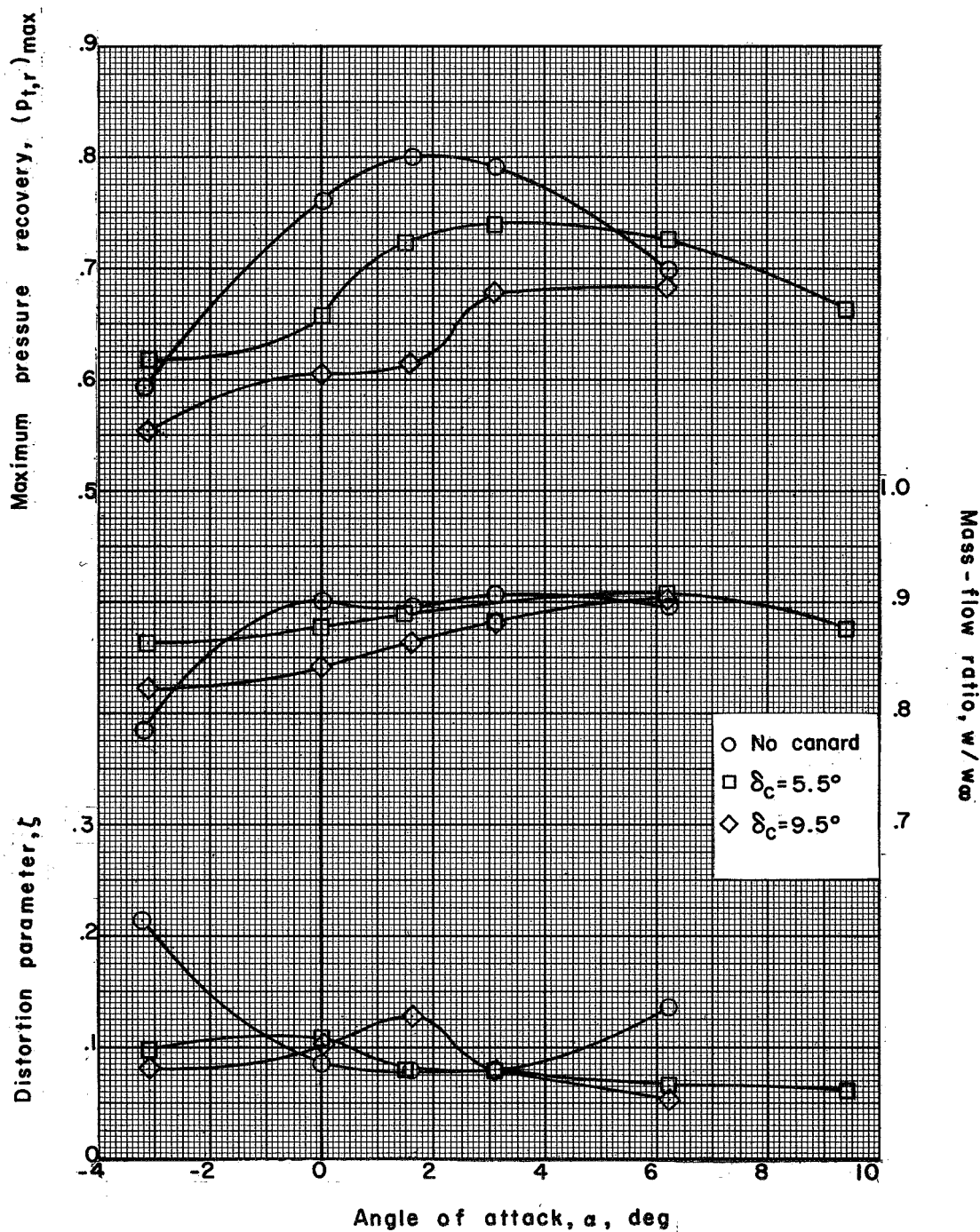
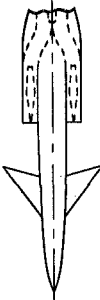
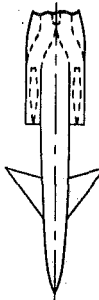
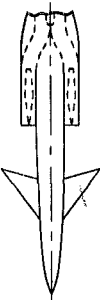
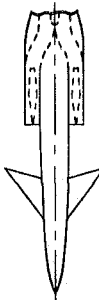


Figure 11.- Effect of canard and canard-control deflection on the induction-system internal-flow characteristics for fuselage 2. Boundary-layer removal system B1; $M = 2.50$.

NOTES: (1) Reynolds number is based on the diameter of a circle with the same area as that of the capture area of the inlet.

(2) The symbol * denotes the occurrence of buzz.

Report and facility	Description			Test parameters				Test data				Performance		Remarks
	Configuration	Number of oblique shocks	Type of boundary-layer control	Free-stream Mach number	Reynolds number $\times 10^{-6}$	Angle of attack, deg	Angle of yaw, deg	Drag profile	Inlet-flow profile	Discharge-flow profile	Flow picture	Maximum total-pressure recovery	Mass-flow ratio	
NASA TM X-464 UPWT		≈6	Perforations in duct wall and central body	1.72 to 2.50	0.83 to 1.41	-4 to 10	0					0.80 at design M = 2.50	0.65 to 1.00*	Two fuselage configurations and flat plates. Tested with and without canard control.
NASA TM X-464 UPWT		≈6	Perforations in duct wall and central body	1.72 to 2.50	0.83 to 1.41	-4 to 10	0					0.80 at design M = 2.50	0.65 to 1.00*	Two fuselage configurations and flat plates. Tested with and without canard control.
NASA TM X-464 UPWT		≈6	Perforations in duct wall and central body	1.72 to 2.50	0.83 to 1.41	-4 to 10	0					0.80 at design M = 2.50	0.65 to 1.00*	Two fuselage configurations and flat plates. Tested with and without canard control.
NASA TM X-464 UPWT		≈6	Perforations in duct wall and central body	1.72 to 2.50	0.83 to 1.41	-4 to 10	0					0.80 at design M = 2.50	0.65 to 1.00*	Two fuselage configurations and flat plates. Tested with and without canard control.

Bibliography

These strips are provided for the convenience of the reader and can be removed from this report to compile a bibliography of NASA inlet reports. This page is being added only to inlet reports.

